Multifractal patterns in the daily catch time series of smooth pink shrimp (*Pandalus jordani*) from the west coast of Vancouver Island, Canada

Rodrigo M. Montes, R. Ian Perry, Evgeny A. Pakhomov, Andrew M. Edwards, and James A. Boutillier

Abstract: There is an urgent need for indicators that anticipate changes in populations of exploited marine species. We modelled the complex patterns of variability found in fisheries time series that are not detected using classical models. We applied fractal analyses to detect time-invariant scaling symmetries in daily catch time series from the smooth pink shrimp (*Pandalus jordani*) fishery from the west coast of Vancouver Island, British Columbia, Canada. A universal multifractal model, which accounts for intermittent fluctuations and extreme values in a time series, provided a better fit to daily catches than a monofractal model. Multifractality is an indication of multiple scaling patterns and suggests that more than one process is affecting the variability of catches. Fractal dynamics in catch time series were found for a range of scales between 16 and 120 fishing days. To our knowledge, this is the first time that multifractality has been demonstrated for an invertebrate fishery. The multifractal model has the potential to provide an in-season estimate (up to 120 fishing days) of the variability of shrimp catches based on the variability at time scales less than 1 month. Changes in these fractal patterns may provide an early warning that conditions underlying this fishery are changing.

Résumé : Il existe un besoin urgent d'indicateurs qui puissent anticiper les changements démographiques des espèces marines exploitées. Nous avons modélisé les patrons complexes de variabilité trouvés dans les séries chronologiques des pêches qui ne sont pas décelés par les modèles classiques. Des analyses fractales nous ont servi à détecter des symétries d'échelle invariables dans le temps dans les séries chronologiques de prises journalières dans la pêche à la crevette océanique (*Pandalus jordani*) sur la côte ouest de l'île de Vancouver, Colombie-Britannique, Canada. Un modèle multifractal universel, qui tient compte des fluctuations intermittentes et des valeurs extrêmes dans la série chronologique, fournit un meilleur ajustement aux prises journalières qu'un modèle monofractal. La multifractalité est une indication de la présence de patrons de cadrage multiples et laisse croire qu'il y a plus qu'un processus qui affecte la variabilité des prises. Nous avons trouvé une dynamique fractale dans les séries chronologiques de prises sur une gamme d'échelles allant de 16 à 120 jours de pêche. À notre connaissance, c'est la première fois que l'on démontre l'existence de multifractalité dans un pêche d'invertébrés. Le modèle multifractal a le potentiel de fournir au cours de la saison (de jusqu'à 120 jours de pêche) des estimations de la variabilité des prises de crevettes basées sur la variabilité à des échelles temporelles de moins d'un mois. Les changements dans ces patrons fractals peuvent fournir un système d'alerte indiquant que les conditions sous-jacentes à cette pêche sont en train de changer.

[Traduit par la Rédaction]

Introduction

Fractal theory has been used in aquatic sciences to quantify scale-invariant relationships under the form of scaling or power laws (Seuront 2010). These scaling laws represent patterns that help to understand the complex structure and organization of marine ecosystems and their populations through space or time (Pascual et al. 1995; Schmid 2000). Under this framework, scale-invariant patterns are detected in a time series by quantifying the dependence between observations and integrating many different temporal scales into a single model. This approach has been proven to be useful in the identification and modelling of ecological and environmental processes that affect the temporal variability of marine planktonic populations (Lovejoy et al. 2001; Fisher et al. 2004).

Received 1 February 2011. Accepted 18 October 2011. Published at www.nrcresearchpress.com/cjfas on 6 February 2012.
J2011-0015

Paper handled by Associate Editor Bernard Sainte-Marie.

R.M. Montes* **and E.A. Pakhomov.** Department of Earth and Ocean Sciences, The University of British Columbia, 6339 Stores Road, Vancouver, BC V6T 1Z4, Canada.
R.I. Perry, A.M. Edwards, and J.A. Boutillier. Fisheries and Oceans Canada, Pacific Biological Station, 3190 Hammond Bay Road, Nanaimo, BC V9T 6N7, Canada.

Corresponding author: Rodrigo M. Montes (e-mail: rmontes@eos.ubc.ca and rmontes@udec.cl).

*Present address: COPAS Sur-Austral, University of Concepción, Casilla 160-C, Concepción, Chile.

In fisheries research, the most common approximations in the statistical modelling of time series involve (*i*) modelling of short-range correlations using univariate (autoregressive integrated moving average, ARIMA) and multivariate (transfer function noise, TFN) models (e.g., Downton and Miller 1998; Hanson et al. 2006) and (*ii*) estimation of short-range correlations (or calculation of the number of independent observations) (e.g., Pyper and Peterman 1998; Perry et al. 2000). The first approach can detect memory patterns at short time scales and can use those patterns to forecast future values, whereas the second approach is often used to adjust the degrees of freedom after conducting classical linear regression and correlation analyses. Both approximations are designed to detect the correlation or dependence between observations that are closely located to each other (i.e., short-range correlations), ignoring the possible dependence that could exist between distant observations (i.e., long-range correlations). Long-range correlations have been detected in fisheries time series (e.g., Halley and Stergiou 2005), but the high variability (intermittency) and nonlinearity usually found in marine catch time series have not been taken into account. These complex dynamics can be quantified in fisheries time series using a framework of long-range correlations developed for studies of turbulence and applied to plankton research (e.g., Seuront et al. 1999; Seuront and Lagadeuc 2001).

Many attempts have been made to detect and model long-range correlations in the field of marine ecology, such as in characterizing the spatial distribution of exploited and non-exploited marine populations and communities (e.g., Azovsky et al. 2000; Guichard et al. 2003). Fractals have been used extensively to model long-range correlations and the intermittent dynamics of marine planktonic and oceanographic time series (e.g., Seuront et al. 1999; Lovejoy et al. 2001; Fisher et al. 2004). However, despite the ability of fractals to integrate multiple time scales of observation in a given model, few examples of their use in modelling marine exploited populations in the time domain can be found in the fisheries literature. Two of these examples are the studies by Halley and Stergiou (2005) and Niwa (2007), who focused on analyzing the dynamics of annual patterns in fishery landings and marine population growth rates, respectively. In a similar way, Niwa (2006) reported long-range correlations in annual recruitment time series of fish populations from the North Atlantic. Since these studies were published, better methods for estimating the degree of long-range correlations for time series on the order of 100 data points (Chamoli et al. 2007) and shorter (e.g., 64 data points, Delignieres et al. 2006) have become available. In addition, methods are now available to estimate how far the effect of long-range correlations are detectable (i.e., extension of scaling ranges; Seuront et al. 2004) quantitatively rather than visually as has been done in previous examples from the fisheries literature.

In the present study, we analyzed the dynamics of fisheries catch time series using a finer scale of temporal resolution (daily) than previous fisheries studies, testing for the existence of multiple scaling patterns (multifractality). We use data on daily catches from the commercial smooth pink shrimp (*Pandalus jordani*) fishery off the west coast of Vancouver Island, British Columbia, Canada, for the period 1994–1996. These data can be considered as long ($N = 642$) because the daily resolution allows for the analysis of intra-annual scales of variability.

Our first objective was to demonstrate the existence of fractal properties in daily fisheries catch time series. Our second objective focused on comparing the monofractal model with the more complex multifractal model regarding their abilities to detect and quantify long-range correlations and high variability. A multifractal model was incorporated into our analysis because it allows the detection of nonlinear and intermittent fluctuations usually found in fisheries time series, in addition to the detection of long-range correlations. Our data come from the commercial smooth pink shrimp fishery off the west coast of Vancouver Island, British Columbia. This fishery was generally open year-round up to 1997 with no quotas from the late 1980s to 1997. The fishery was conducted by small vessels using otter and beam trawls, with footrope lengths between 9 and 27 m and vertical openings greater than 1.5 m (Perry et al. 2000; Rutherford et al. 2004). *Pandalus jordani* is a protandric hermaphrodite species that generally lives up to 3 years, rarely up to 4 years. This means that they spawn first as males and then change their sex to females around 2 years of age (Butler 1980). Spawning occurs during the fall–winter period, and the eggs hatch during the spring (Butler 1980). Individuals fully recruit to the fishery at the age of 2 years (Boutillier et al. 1997).

We start with a basic introduction to fractals and long-memory processes and then analyze the pink shrimp trawl fishery data for the presence of these long-range correlations and intermittent dynamics. We conclude by discussing some hypotheses that may explain the observed patterns of variability. We also discuss the potential for this approach to be used to assist with the management of this fishery and to develop early warning indicators of changes in the underlying environmental or human processes within which this fishery operates.

Materials and methods

Fractals and long-memory processes

A fractal can be defined as an object that lacks a characteristic length because the same geometrical structures are present at all length scales. If the observational scale is reduced, new structures arise, and the new ones are similar to those of the original unit. As a consequence, fractals are composed of subunits (and further subunits) that resemble the larger scale structure, a property known as self-similarity (Mandelbrot 1983; Goldberger et al. 2002). Self-similar processes are invariant in distribution under scaling of space and (or) time, and the scaling coefficient (or index of self-similarity) is a positive number denoted H (the Hurst coefficient; Samorodnitsky and Taqqu 1994). Here, $0 < H \leq 1$. Because of this property, the shape of fractals is nonrectifiable, meaning that they consist of an infinite sequence of clusters within clusters or waves within waves. In rectifiable objects, increasingly accurate measurements based upon successively smaller scales converge to a limit that is the true extent (length) of the object (Mandelbrot 1983). However, in fractals, the same procedure generates an infinite series according to a power law:

$$(1) \qquad \lambda(r) = kr^{1-D}$$

where λ is the length of the object measured at the scale unit r (the length of the object diverges as $r \to 0$), k is a constant, and D is the fractal dimension (the definitions of all variables are summarized in Table 1). D exceeds the topological dimension (d) of an object and is not an integer and satisfies $d < D < d + 1$, where $d + 1$ is the space dimension of the object. For example, for a fractal time series, $1 < D < 2$, and $D = 2 - H$.

Fractal (or scale-invariant) processes have no characteristic scale, which means that all scales contribute to the observed dynamics. This property is referred as a scaling law or scaling behavior (Abry et al. 2009). Fractal processes generate irregular fluctuations on multiple time scales, analogous to fractal objects that have a wrinkle structure on different length scales (Mandelbrot 1983). In an idealized model, scale-invariance holds on all scales, but the real world imposes upper and lower bounds over which such behavior applies (Goldberger et al. 2002).

In contrast with monofractals, which are homogeneous in the sense that they have the same scaling properties characterized by only one exponent or coefficient (i.e., H) throughout the entire signal, multifractals are a class of signals that requires a large number of indices to characterize their scaling properties. Multifractal signals are intrinsically more complex and inhomogeneous than monofractals (i.e., different parts of the signal may have different scaling properties; Goldberger et al. 2002). Monofractal analysis looks at the geometry of a pattern, whereas multifractal analysis looks at the arrangements of quantities. A monofractal can be defined as a geometrical set of points and a multifractal is defined as a mathematical measure (Lavallée et al. 1993). The multifractal approach implies that a statistically self-similar measure can be represented as a combination of interwoven monofractal sets with corresponding scaling exponents. A combination of all the monofractal sets produces a multifractal spectrum that characterizes variability and heterogeneity of the analyzed variable (Kravchenko et al. 1999). In this study, to determine whether a monofractal or a multifractal model better describes pink shrimp daily catches, we used an objective statistical procedure that has not been applied previously in this context.

One means of capturing long-range correlations or long-memory features of fractal time series is with self-similar stochastic processes, also known as stochastic fractals (Mandelbrot 1983; Samorodnitsky and Taqqu 1994). A long-memory process has an autocovariance function with a decay rate much slower than the decay rate characteristic of a standard stationary autoregressive process (Percival et al. 2001). In other words, the observations separated by long time intervals still exhibit a nonzero covariance (current observations retain some "memory" of distant past observations). Self-similar models have been studied for more than three decades and have been successfully applied in a variety of fields in the form of fractional Gaussian noise (fGn) and fractional Brownian motion (fBm) (e.g., Mandelbrot and Van Ness 1968; Rodriguez-Iturbe and Rinaldo 2001). For self-similar time series, the Hurst coefficient (H) is a measure of long-range dependence. When $H > 0.5$, all the observations of a time series are positively correlated, and the closer H is to 1 the smoother the function. When $H < 0.5$, all observations are negatively correlated. A time series having the characteristics of Gaussian white noise corresponds to an fGn series with $H = 0.5$ (Samorodnitsky and Taqqu 1994). fGn corresponds to a stationary process with constant mean and variance, whereas fBm is nonstationary with stationary increments (Mandelbrot and Van Ness 1968). Differencing fBm creates fGn, and cumulatively summing fGn produces fBm. Both processes are characterized by the same Hurst coefficient but display different dynamics.

Pink shrimp fishery and total daily catches

Smooth pink shrimp are captured by the trawl fishery with six other species of shrimp, and up to 1996, the majority of the catch was a mix of smooth pink shrimp (greater than 90%) and sidestripe shrimp (*Pandalopsis dispar*) (Rutherford et al. 2004). Individual trawls (mass of shrimp in kilograms for each trawl) for *P. jordani* were obtained from Fisheries and Oceans Canada. This time series takes into account otter and beam trawls and is from offshore Pacific Fisheries Management Areas (PFMA) 121, 123, 124, and 125 (Fig. 1). Catch data were recorded by fishermen in harvest logbooks at the time of fishing.

A total daily catch (TDC: the daily sum of recorded catches) time series was constructed for the west coast Vancouver Island smooth pink shrimp fishery for the 1994–1996 period. Only individual trawls registered during the principal spring–summer fishing season (April–October; Perry et al. 2000) were used, giving 214 days each year. No major fishing activity was recorded during the November–March period of each year. In consequence, sporadic days with trawling activity during this latter period were not considered as fishing days and were not included in this study. Total daily catches for the three years were "stitched" together to yield a total of 642 fishing days (Fig. 2); the consequences of the stitching will be discussed later. This time series corresponds to the longest period of total daily catches from the main fishing season for which the smallest number of days with no observations occurred (24 "missing" observations, equivalent to 3.7% of the total). Missing observations were estimated by linear interpolation using one point on either side of the missing value. Interpolations can add correlations to time lags less than 30 data points for time series with 10% of missing data filled by linear interpolations (Wilson et al. 2003). In our case, as the percentage of missing observations is less than 5%, we expect to find the effect of spurious correlations (if any are present) at scales significantly less than 1 month.

The pink shrimp TDC time series presented a marked periodicity and a slight increasing linear trend (Fig. 2). Its periodogram (not shown) has a strong peak at a frequency (0.0047 fishing days^{-1}) equivalent to the period of one fishing season (214 fishing days). This corresponds to an annual cycle (summer to summer) owing to the stitching together of the 3 years of data. Periodicities are considered as deterministic trends that can obscure the detection of scaling behaviour, and as such they must be removed before the estimation of long-memory parameters (Montanari et al. 1999). First, the linear trend of the TDC time series was removed by a least squares fit ($R^2 = 0.04$, $p < 0.01$). The seasonal period corresponding to the annual cycle (frequency

Table 1. Definitions of variables and parameters used in the text.

Symbol	Definition
H	Hurst coefficient
C_1	Intermittency parameter
α	Lévy index
λ	Length of a fractal object
r	Time lag or scale unit (fishing days)
k	Constant of power law equation
D	Fractal dimension
d	Topological dimension ($d = 1$ for time series)
u_i	Total daily catch observations of the linearly detrended time series
a_0; a_j, b_j	Intercept and amplitudes of Fourier series
j	Fourier index
i	Daily values index
$E(w)$	Spectral power
w	Frequency
q	Statistical moment
β	Power spectrum slope
x_i	Value of the TDCa* time series for day i
$Y_r(q)$	Structure function empirical observations
$\hat{Y}_r(q)$	Structure function fitted values
N	Total length of pink shrimp catch time series
$\zeta(q)$	Structure function scaling exponent
$H(q)$	Hierarchy of Hurst coefficients
$K(q)$	Scaling moment function
U	Theil's inequality coefficient
r_1	Lower scaling limit
r_2	Upper scaling limit
R'	Deviance
p_1	Number of parameters of monofractal model
p_2	Number of parameters of multifractal model
α'	Significance level

*TDCa is the total daily catch anomaly time series obtained after cumulatively summing the TDCr time series, where TDCr represents the total daily catch residual time series.

equal to 0.0047 fishing days^{-1}) and its first harmonic (frequency equal to 0.0093 fishing days^{-1}), which in total explained 25% of the time series variance, were identified in the resulting TDC linearly detrended time series by fitting a Fourier series using the following equation:

$$(2) \qquad u_i = a_0 + \sum_{j=1}^{m} a_j \cos\left(\frac{2\pi i}{j}\right) + b_j \sin\left(\frac{2\pi i}{j}\right)$$

where

$$a_j = b_j = \frac{2}{N}\sum_{i=1}^{N} u_i \cos\left(\frac{2\pi ij}{N}\right)$$

Here, $\cos(2\pi i/j)$ and $\sin(2\pi i/j)$ are used, for a fixed frequency, as predictor variables to fit the intercept a_0 and the amplitudes a_j and b_j from the data u_i using an ordinary least squares regression method (Cryer and Chan 2008). The time series of residuals obtained after the elimination of deterministic trends is hereafter called the TDC residual time series (TDCr). A step-by-step diagram showing all transformations conducted on the pink shrimp TDC time series is provided (Fig. 3). The above linear detrending procedure and the removal of seasonal components are Step 1.

For Step 2, nonstationary segments in the TDCr time series were removed as they tend to give a biased estimate of H near 1 (Yu et al. 2003). After that, the mean of TDCr was subtracted from the individual values, and the cumulative sum (partial summation) of the obtained values was calculated (e.g., Gao et al. 2006). The series obtained after this operation is hereafter called the TDC anomaly time series (TDCa). The TDCa time series is free of periodicities and is nonstationary, as is required to estimate the multifractal parameters.

Monofractal and multifractal analysis

Scaling dynamics and stationarity were tested using power spectrum analysis (Davis et al. 1994; Rodriguez-Iturbe and Rinaldo 2001). If scaling is present in pink shrimp catches, the characteristic power-law form of fractals will appear as

$$(3) \qquad E(w) \approx w^{-\beta}$$

where w is frequency, $E(w)$ is the power of the TDCa time series (squared modulus of the fast Fourier transform; Davis et al. 1996), and β an exponent to be estimated. On a logarithmic scale, scaling dynamics will manifest as an approximately linear curve when plotting $E(w)$ versus w. Power spectrum analysis is equivalent to an analysis of variance in which the total variance (statistical moment $q = 2$) is partitioned into contributions coming from processes with differ-

Fig. 1. Fisheries and Oceans Canada Pacific Fishery Management Areas (PFMA). Data for this study came from PFMA 121, 123, 124, and 125 off the west coast of Vancouver Island, British Columbia, Canada.

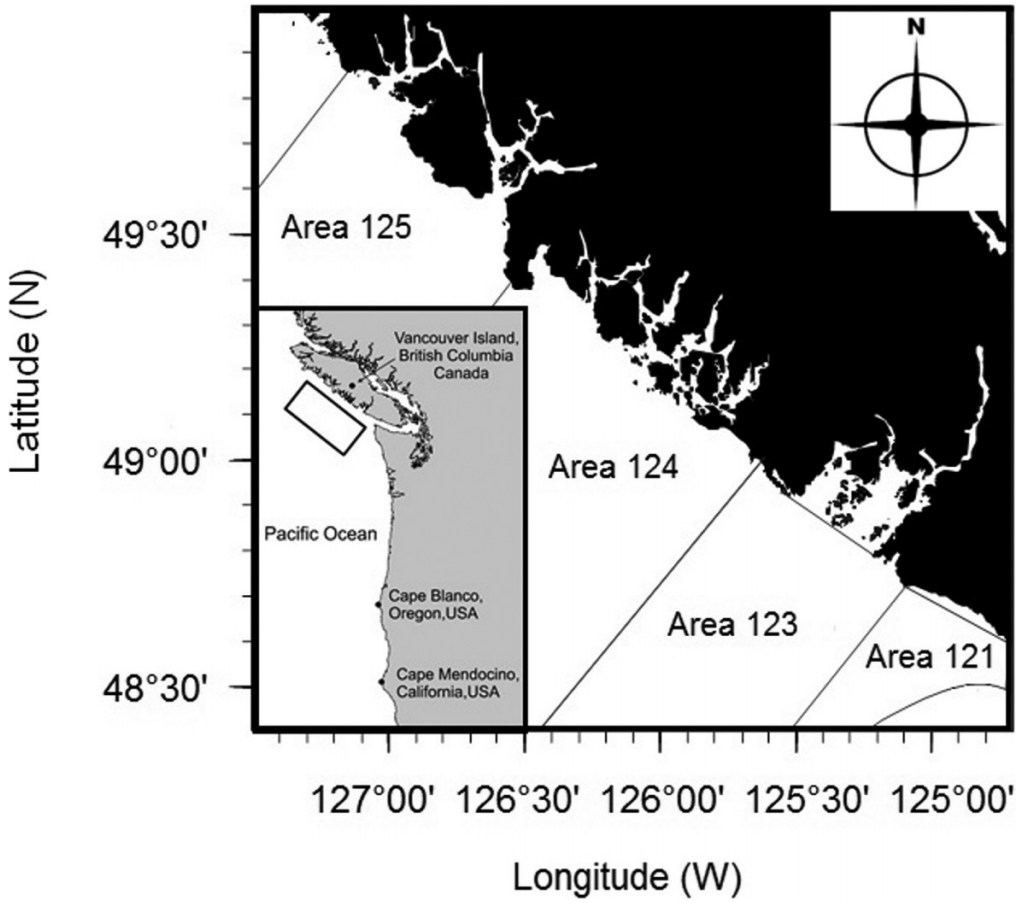

Fig. 2. Pink shrimp *(Pandalus jordani)* total daily catch (i.e., daily sum of all recorded catches; TDC) time series from 1994 to 1996 for the April–October period (642 fishing days) in Pacific Fishery Management Areas 121, 123, 124, and 125, west of Vancouver Island, Canada. A sinusoidal curve with an annual period of 214 fishing days was fitted to this time series. A slightly increasing linear trend is also visible in this time series.

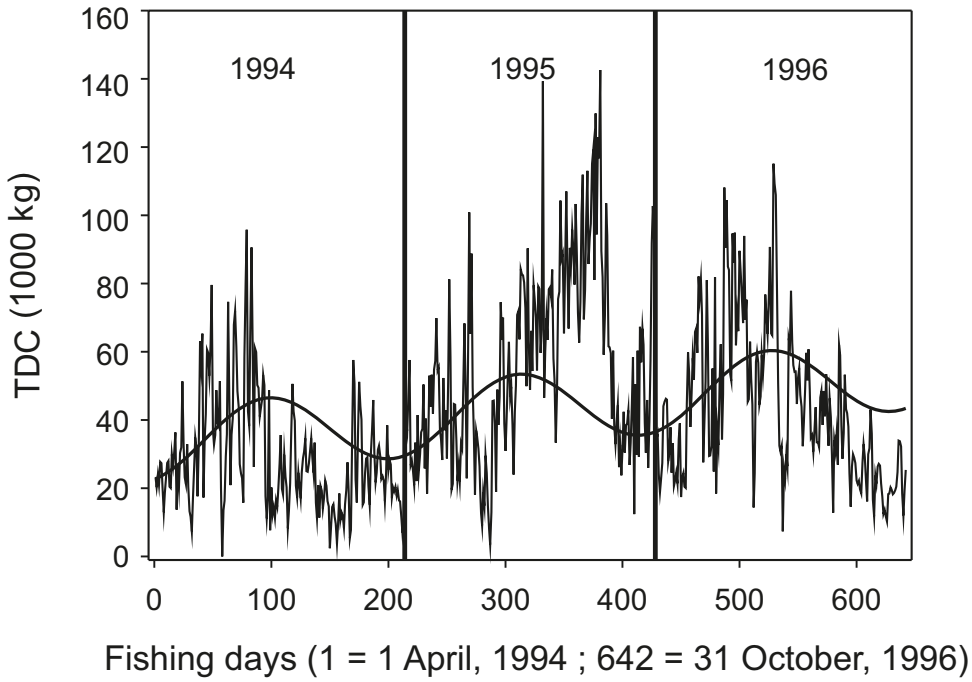

Fig. 3. Diagram showing the transformations and mathematical operations conducted on pink shrimp (*Pandalus jordani*) total daily catch time series (TDC) on a step-by-step basis. TDCr represents the total daily catch residual time series, and TDCa is the total daily catch anomaly time series obtained after cumulatively summing the TDCr time series.

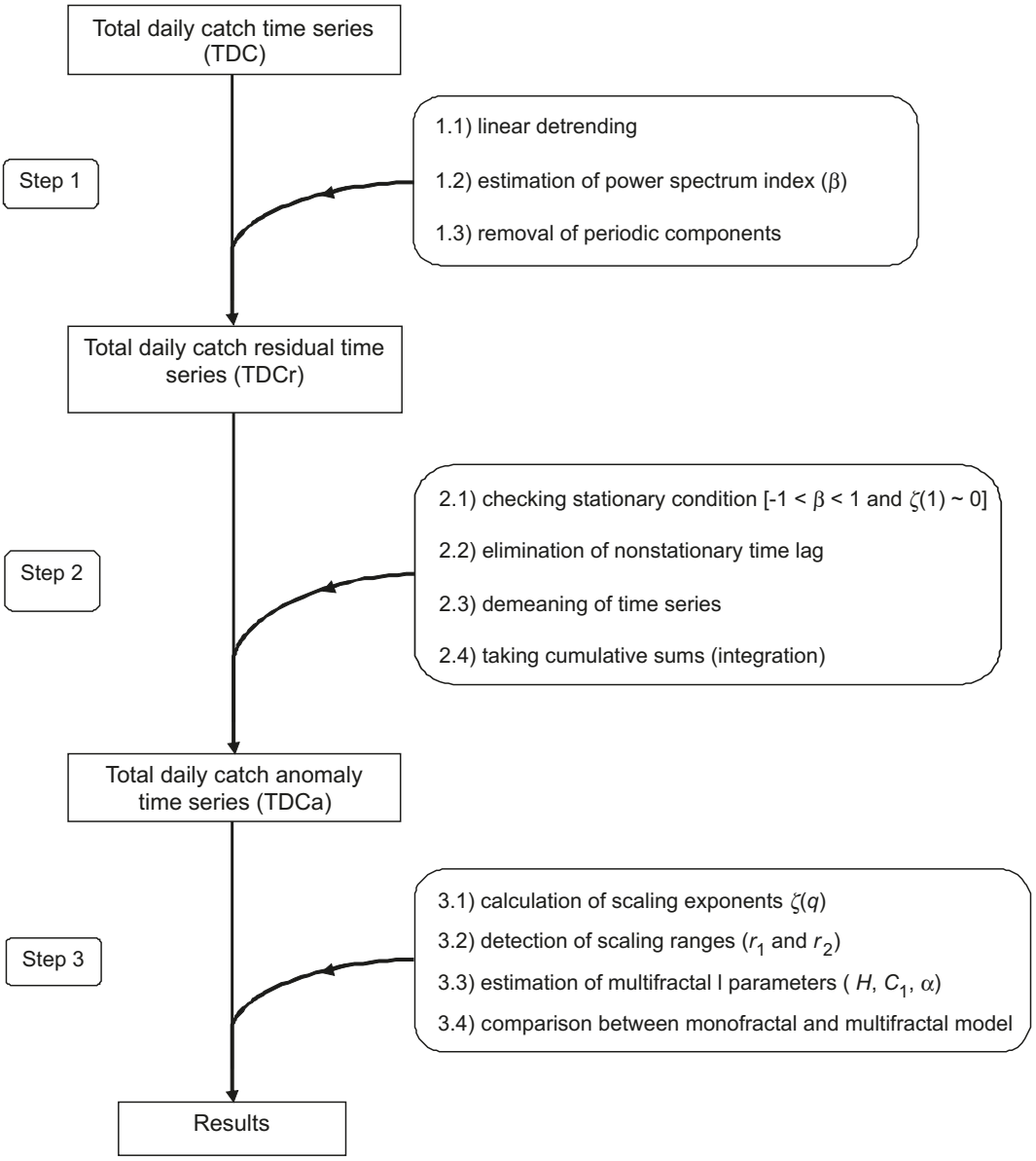

ent time scales giving a quantitative measure of the importance of each frequency (Seuront et al. 1999). As a consequence, highly intermittent and non-Gaussian time series are not appropriately quantified using this methodology, which focuses only on the second-order moment (Seuront and Lagadeuc 2001).

To completely quantify the scaling dynamics of the TDCa time series, we analyzed higher statistical moments using a function of order q (statistical moment) known as a structure function (Davis et al. 1996; Tennekoon et al. 2005) or generalized variogram (Lavallée et al. 1993; Rodriguez-Iturbe and Rinaldo 2001). When $q = 2$, the structure function corresponds to the variogram (Davis et al. 1994). Structure functions are only applicable to nonstationary self-similar time series (Davis et al. 1994; Yu et al. 2003) (i.e., a time series for which the slope β obtained from eq. 3 fluctuates between $1 < \beta < 3$). These time series correspond to nonstationary processes with stationary increments (Davis et al. 1994, 1996). However, if $-1 < \beta < 1$, the time series is classified as strictly stationary, and a transformation to convert it to a nonstationary process is necessary before using structure functions (Yu et al. 2003; Gao et al. 2006). These functions have been used in plankton ecology (e.g., Seuront et al. 1999; Fisher et al. 2004) and were also applied in the analysis of the multifractal temporal dynamics of the southern hake (*Merluccius australis*) fishery of Chile (Montes 2004). The structure function $Y_r(q)$, for time lag r and statistical moment q, is defined as

$$(4) \qquad Y_r(q) = \left\langle |(x_{i+r}) - (x_i)|^q \right\rangle; \quad r = 1, 2, 3, \ldots, N/4$$

where N is the length of the TDCa time series, x_i is the value of the TDCa time series for day i, and the operator $\langle \ldots \rangle$ cor-

responds to the mean over $i = 1, 2, 3, \ldots, N - r$. The time lag r is equivalent to the scale unit defined in eq. 1 and is measured using previously defined fishing days. The maximum time lag r is usually set to $N/2$ because a greater time lag is more affected by low sample sizes and also by spurious properties of the data (Journel and Huijbregts 1978). To be conservative, in this study the maximum time lag r was set to $N/4$. In the averaging procedure, we considered 482 pairs of data from the TDC residual time series, which is significantly more than the 100 data pairs (Tennekoon et al. 2005) or 225 data pairs (Webster and Oliver 1992) considered reliable when structure functions or their equivalent variograms are calculated.

The scaling exponents $\zeta(q)$ were estimated by the slope of the linear regression between $Y_r(q)$ and r on a logarithmic scale for different statistical moments q using the following equation:

$$(5) \qquad Y_r(q) \approx r^{\zeta(q)}$$

We considered 40 moments in the structure function calculations, such that q varies between 0.1 (weakest and most frequent fluctuations) and 4.0 (strongest but sporadic fluctuations) with an increment of 0.1. We then define a hierarchy of Hurst coefficients using the $\zeta(q)$ values as

$$(6) \qquad H(q) = \frac{\zeta(q)}{q}$$

which is the goal of this method (Davis et al. 1994). Those processes with constant $H(q)$, characterized by simple scaling, are known as monofractals (or simple fractals). Processes with nonlinear and convex (downward facing) $\zeta(q)$ are called multifractals (Seuront et al. 1999; Tennekoon et al. 2005). For monofractals, $\zeta(q)$ is linear (e.g., $\zeta(q) = q/2$ for Brownian motion). In particular, the first moment ($q = 1$) gives the scaling exponent $H = \zeta(1)$, corresponding to the scale dependency of the average fluctuations. If $H \neq 0$, the fluctuations $Y_r(q)$ will depend on the time scale, which characterizes the degree of stationarity of the process (Seuront and Lagadeuc 2001). No scaling is present for a strictly stationary process $\zeta(q) \sim 0$, and therefore structure functions are also used to detect stationary (and nonstationary) segments in a time series before the estimation of multifractal parameters (Yu et al. 2003).

We used the Universal Multifractal Model (Schertzer and Lovejoy 1987; Lovejoy et al. 2001) to characterize and quantify the dynamics of a multifractal process. In using this model we avoided estimating a large number of exponents, $\zeta(q)$, to completely characterize the dynamics of the pink shrimp catch time series. Under this framework, the multiscaling behavior of an intermittent process can be quantified using a scaling moment function $K(q)$, which depends only on two parameters, C_1 and α, estimated through

$$(7) \qquad K(q) = \begin{cases} \dfrac{C_1}{\alpha - 1}(q^\alpha - q); & \alpha \neq 1 \\ C_1\, q \log(q); & \alpha = 1 \end{cases}$$

The intermittency parameter C_1 characterizes the heterogeneity of the process; when this parameter increases, the magnitude of sudden large jumps increases (Seuront and Lagadeuc 2001). It is also known as the codimension (i.e., the fractal dimension is $d - C_1$; $d = 1$ for time series). A value of C_1 near 0 indicates a process (in this case, a time series) having near-average observations at all times (homogenous), whereas a value of C_1 near 1 corresponds to a process that usually has very small observations except on rare and distant occasions when an observation significantly exceeds the average (i.e., heterogeneous or sparse) (Seuront and Lagadeuc 2001). It goes beyond the standard concept of asymmetry known as skewness (which only looks at the third statistical moment) and has a long-term memory signature (Seuront 2010). The parameter α, also known as the Lévy index, measures the degree of multifractality and determines the shape of the probability distribution; it satisfies $0 < \alpha \leq 2$ (Seuront et al. 1999). As α decreases, the frequency of sudden large jumps increases.

For a multifractal, the departure from the simple linear behaviour can be quantified by extending eq. 7 to include the scaling function $K(q)$ as

$$(8) \qquad \zeta(q) = qH(q) - K(q)$$

where $H(1) = \zeta(1)$ is the Hurst exponent for the monofractal case. For monofractals (i.e., when $C_1 = 0$ or $\alpha = 0$), $\zeta(q)$ is a linear function of q. In the present study, H, C_1, and α were estimated in Step 3 by the nonlinear regression of eq. 7 (e.g., Seuront et al. 2002; Tennekoon et al. 2005).

Estimation of confidence intervals

We used a nonparametric bootstrap procedure in which the residuals obtained from the fit of the nonlinear regression to the Universal Multifractal Model (eq. 8) were randomized (e.g., Crawley 2007). The 95% confidence intervals (Efron and Tibshirani 1993) were estimated using 1000 resamples. Calculations were performed using R software (version 2.7.2, R Development Core Team 2005).

Detection of scaling ranges

Scaling ranges were detected on Step 3 using three different criteria: local slopes, zero slope, and "R^2-SSR" (Takalo et al. 1995; Seuront et al. 2004).

First, we used an automatic adaptive scaling range selection algorithm (Xia et al. 2005), which finds the linear region of a curve by comparing how closely a linear regression model characterizes the observed data points. It uses an independent measure of goodness of fit known as Theil's inequality coefficient, U (Theil 1972), which is calculated as

$$(9) \qquad U = \frac{\sqrt{\frac{1}{N^*}\sum_{r=1}^{N^*}(\hat{Y}_r - Y_r)^2}}{\sqrt{\frac{1}{N^*}\sum_{r=1}^{N^*}(\hat{Y}_r)^2} + \sqrt{\frac{1}{N^*}\sum_{r=1}^{N^*}(Y_r)^2}}$$

where $\hat{Y}_r$ are the values fitted by the linear model, Y_r correspond to the structure function values, and N^* is the sample size for U equivalent to $N/4$. The observed time scale or time lag r was measured with increments of 1 fishing day. The denominator of eq. 9 is used to normalize U between 0 and 1. As U approaches zero, the fitted data points get closer to the observed data. To determine scaling breaks, we used a threshold value of U equal to 0.015 as estimated between two time scales r_1 and r_2 (Xia et al. 2005). The initial starting

Fig. 4. Power spectrum of the pink shrimp (*Pandalus jordani*) total daily catch time series (TDC) off the west coast of Vancouver Island for 1994–1996. The fitted straight line is a preliminary indication of scaling.

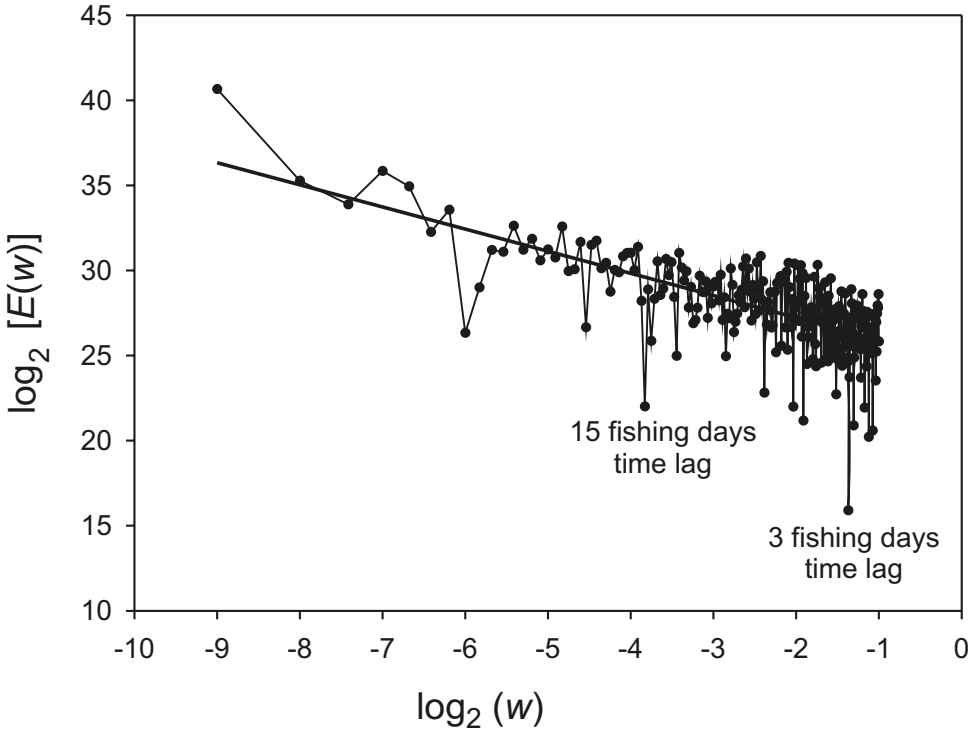

point for the algorithm was set as the middle region of the curve (i.e., $r_1 = (N^*/2) - 1$ and $r_2 = (N^*/2) + 1$).

Second, to check the consistency of the scaling range selected with the Xia et al. (2005) algorithm, local slopes of Y_r were calculated between adjacent data points and plotted as a function of time lag r on a logarithmic scale. If the time series is self-similar, local slopes should be approximately constant for some time period (Takalo et al. 1995), which is equivalent to the so called "zero-slope" criterion used by Seuront et al. (2004). This criterion was designed to detect a difference between the slope of a regression line and a theoretically expected slope of zero using a t test (Zar 1999). Finally we applied the "R^2-SSR" criterion (Seuront et al. 2004), which determines the scaling range maximizing the coefficient of determination (R^2) and minimizing the total sum of squared residuals (SSR) of the regression line.

Selection between monofractal and multifractal models

To determine whether structure function observations calculated using eq. 4 are better fitted by a monofractal than a multifractal model, or vice versa, visual detection is generally used. This is done by visually comparing the fits of the theoretically fitted monofractal curve (straight line) and the fitted multifractal curve (dome shaped curve) with the observations. However, we used the likelihood ratio test for nested models (Burnham and Anderson 2002) to select the model that best describes the structure function observations. By setting $C_1 = 0$ or $\alpha = 0$ in eq. 8 for the multifractal model, we obtained the monofractal model $\zeta(q) = qH$, denoted as M_1, which is a nested model of the multifractal model M_2. Assuming normal errors with constant variance, the statistic R' (Hilborn and Mangel 1997), which represents twice the difference in negative log-likelihoods given the data, also called the deviance, was calculated as

$$R' = 2[\log L(\mathrm{M}_2|\mathrm{data}) - \log L(\mathrm{M}_1|\mathrm{data})] \quad (10)$$

where $L(M_k|\,\mathrm{data})$ is the likelihood of model k. R' has a χ^2 distribution with $p_2 - p_1$ degrees of freedom, where p_1 and p_2 are the number of parameters of M_1 and M_2, respectively; here, $p_2 - p_1 = 2$. If R' is greater than χ^2 at the $\alpha' = 0.05$ level, then the multifractal model is significantly better than the monofractal model at this level.

Results

Scaling of TDC and stationarity of TDCr time series

A preliminary indication of scaling over multiple ranges was obtained by fitting a straight line through the power spectrum plot of the linearly detrended TDC time series (Fig. 4). However, there was significant variability in this plot, especially at both ends of the spectrum, which means that it was not possible to detect clear scaling breaks that can be used to estimate monofractal parameters. This power spectrum analysis is only used here as a preliminary assessment of scaling in the TDC time series (Step 1, Fig. 3) and to classify the TDCr time series as stationary or nonstationary (Step 2, Fig. 3).

The slope ($-\beta$) obtained from the power spectrum analysis (eq. 3) is equal to –0.37, which means that the TDCr time series corresponds to a stationary process (Davis et al. 1994). A more detailed analysis using structure functions revealed the existence of two increasing trends in TDCr time series: the first between 1 and 3 fishing days and the second between 4 and 15 fishing days (Fig. 5). These scaling breaks

Fig. 5. Structure function $Y_r(q)$ versus r in a log–log plot obtained from the pink shrimp (*Pandalus jordani*) total daily catch residual time series (TDCr) for the west coast of Vancouver Island from 1994 to 1996. Two increasing trends, the first between 1 and 3 fishing days and the second between 4 and 15 fishing days, are visible.

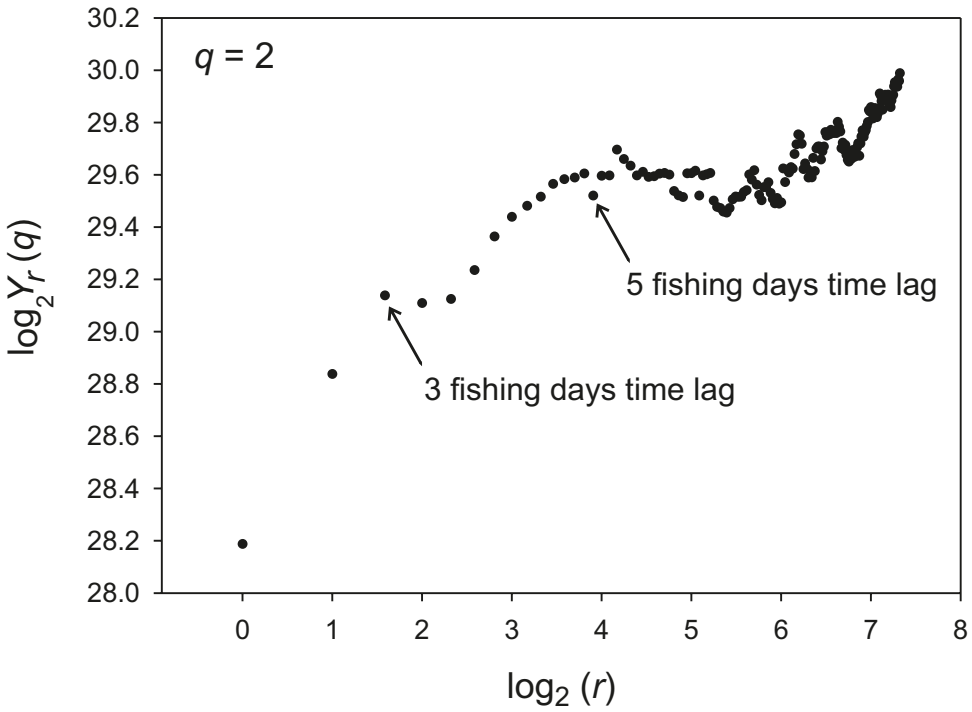

are in agreement with those observed in the power spectrum plot of the TDC time series at the same time lags (Fig. 4). Therefore, the nonstationary segment over the range from 1 to 15 fishing days was excluded before the estimation of multifractal parameters (Step 2 of Fig. 3). This latter procedure avoids a biased estimation of the Hurst coefficient because of the spurious effects of trends on the self-similar properties of total daily catches. This means that 16 fishing days was selected as the lower limit before the detection of scaling ranges. For the TDCr time series, we obtained a value of $H = \zeta(1) = 0.05$, after excluding the initial nonstationary segment, which confirms (*i*) that TDCr is close to a strict stationary process for which $H = \zeta(1) = 0$ and (*ii*) the need to take cumulative sums of (integrate) the TDCr time series before calculating the structure functions. As explained in the Methods section, taking cumulative sums is necessary when a time series is analyzed as a random walk and $H = \zeta(1)$ is close to zero (Gao et al. 2006). The integrated TDCr time series forms the total daily catch anomaly time series (TDCa), and the latter is used hereafter in the calculation of scaling ranges and in the estimation of multifractal parameters.

Selection of scaling ranges

Xia et al.'s (2005) adaptive search algorithm applied to detect the linear region of the curve using structure function values $Y_r(q)$ for $q = 1$ selected a scaling range of 16 to 120 fishing days (Fig. 6). The value of Theil's inequality coefficient U obtained from eq. 8 for the selected scaling range was 0.0001, which is far below the threshold value of $U = 0.015$. A value of $R^2 = 0.99$ ($p < 0.01$) confirmed the good fit of the linear regression model for this scaling range. According to the second criterion for detecting scaling ranges, local slopes were plotted against the time lag and a zero slope was obtained for several regression lines. These lines have a fixed lower scaling limit of 16 fishing days and an upper scaling limit that varied between 116 and 129 fishing days. After approximately 120 fishing days, local slopes generally decreased, showing the absence of a scaling region after that time lag (Fig. 7).

The response of structure functions to the presence of periodic oscillations is well known. In these cases, structure functions reach their maximum values at half of their period and their minimum values at the time scale of their period (Takalo et al. 1995; Yu et al. 2003). After stitching together the data points of the total daily catch time series from the main fishing seasons from 1994 to 1996, a period equal to 214 fishing days was artificially created. The structure function for the TDCr time series reaches a value near its maximum at 214 fishing days, which demonstrates that the main seasonal period of 214 fishing days was efficiently removed and has no effect on the structure function plot. Using the "R^2-SSR" criterion and a lower scaling limit of 16 fishing days, we obtained a maximum coefficient of determination ($R^2 = 0.9978$) and a minimum sum of squared residuals (SSR = 0.0475) for a regression line with zero slope ($t = 0.621$, $p < 0.01$) at a time lag equal to 120 fishing days. In conclusion, lower and upper scaling limits of 16 and 120 fishing days were used to estimate monofractal and multifractal parameters.

Estimation of monofractal and multifractal parameters and selection of models

Structure functions for the TDCa time series exhibit linear trends over the selected scaling range (16 to 120 fishing days according to Xia et al.'s (2005) algorithm) for all statistical

Fig. 6. Scaling range (between 16 and 120 fishing days) selected by the adaptive search algorithm (Xia et al. 2005) applied to detect the linear region of the structure function curve of the total daily catch anomaly time series (TDCa) for $q = 1$. Upper scaling limit is marked by an arrow. Inset shows a close-up view of the departure of the structure function from the linear trend at 120 fishing days.

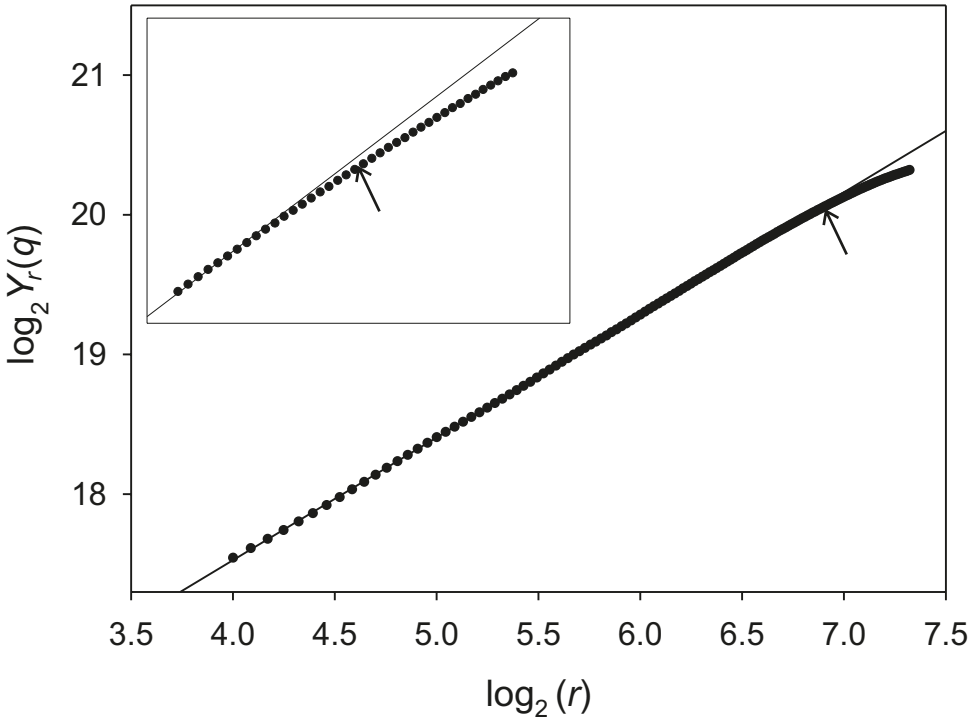

Fig. 7. Temporal variability of local slopes calculated for TDC anomaly time series (TDCa) for time lags between 16 and 321 fishing days. Local slopes fluctuate around a constant value up to approximately 120 fishing days and notably decrease after that.

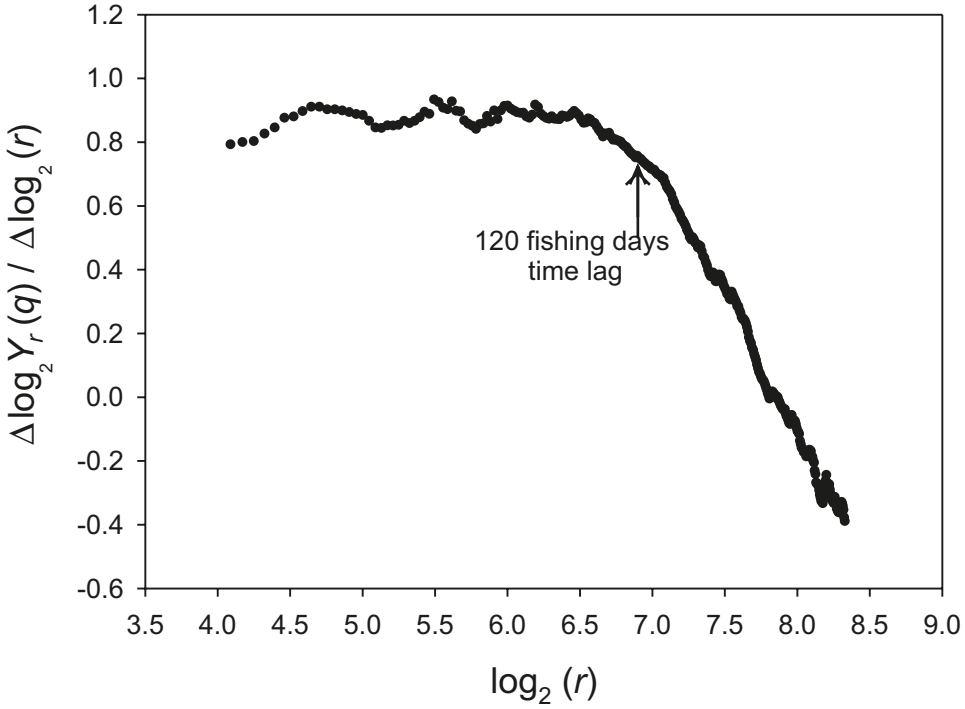

moments. For clarity, only four moments ($q = 1, 2, 3, 4$) from a total of 40 are shown (Fig. 8). The value estimated for H was 0.8779 (95% confidence interval (CI): 0.8777, 0.8783). This value can also be obtained using eq. 6 for which $H = \zeta(1) = 0.8778$, which is very close to the value from the nonlinear regression model. The empirical structure function calculated using the exponents $\zeta(q)$ for q between 0.1 and 4.0 is nonlinear, which means that the TDCa time series is multifractal over the selected scaling ranges (Fig. 9). The empirical and theoretical multifractal curves

Fig. 8. Structure function $Y_r(q)$ versus r in a log–log plot obtained from the pink shrimp (*Pandalus jordani*) total daily catch anomaly time series (TDCa) for the west coast of Vancouver Island from 1994 to 1996. A linear trend selected by the adaptive search algorithm (Xia et al. 2005) for $q = 1$ in Fig. 6 is visible also for statistical moments $q = 1, 2, 3, 4$ for a range of scales from 16 to 120 fishing days marked between vertical dashed lines.

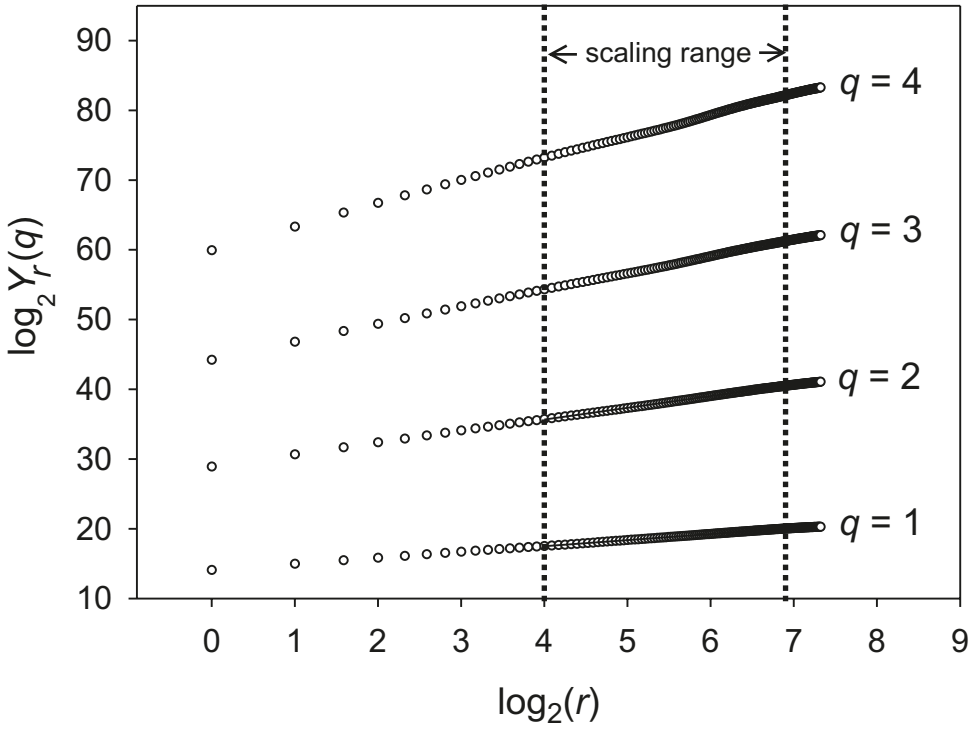

Fig. 9. Empirical curve for scaling exponents, $\zeta(q)$, (solid circles) compared with the monofractal curve $\zeta(q) = qH$ (continuous line) and with the theoretical universal multifractal function (crosses) obtained from the pink shrimp (*Pandalus jordani*) total daily catch anomaly (TDCa) time series with $H = 0.8779$, $C_1 = 0.0429$, and $\alpha = 1.5073$.

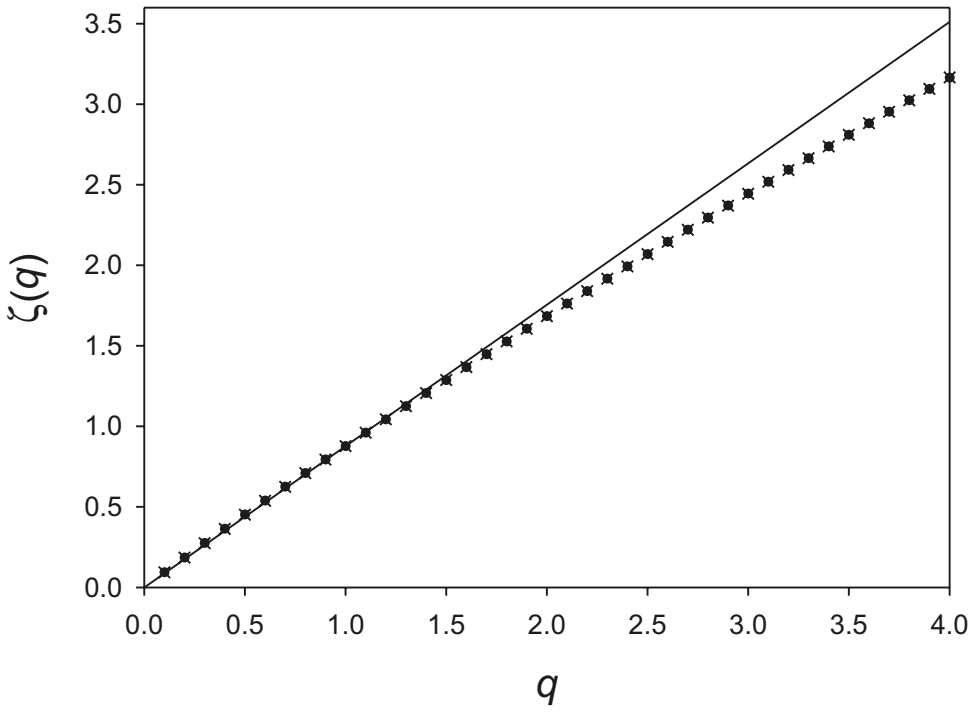

also showed good agreement (Fig. 9) when the theoretical curve was calculated using the estimated universal multifractal parameters $C_1 = 0.0429$ (95% CI: 0.0425, 0.0435) and $\alpha = 1.5073$ (95% CI: 1.493, 1.521). Since the TDCa time series is multifractal, $H = \zeta(1)$ cannot be interpreted as a Hurst coefficient because multiple scaling patterns are re-

quired to characterize the dynamics of this time series. This means that a single coefficient (H) cannot determine the complete statistical scaling features of the TDCa time series, and additional parameters (C_1 and α) are necessary to explain the variability. For this case, the Hurst coefficient is estimated using the Lévy index as $H = 1/\alpha$ (Samorodnitsky and Taqqu 1994), which is equal to 0.66.

The estimated R' statistic from the likelihood ratio test obtained from eq. 10 was 362; this is much greater than 5.99, the value calculated at the $\alpha' = 0.05$ significance level. This test clearly selected the multifractal over the monofractal model, which confirms the good fit of the theoretical multifractal model to the empirical multifractal observations shown in Fig. 9. However, more observations will be necessary to make multifractal models a useful tool in the forecasting of total daily catches in fisheries research. This is because the error introduced in using finite length time series for the estimation of scaling exponents using structure functions is less than 5% if the minimum number of data points varies between 1000 and 3000 according to the dynamics of the time series (Kiyani et al. 2009). This does not mean that the TDCa time series is not multifractal. This only means that our estimation of multifractal parameters could have been affected by the limited number of observations available, and in consequence when using structure functions and a multifractal model to forecast TDC values, no less than 3000 observations should be used.

Discussion

Identification of multifractal patterns

To our knowledge, this is the first time that multiscale temporal patterns of variability (i.e., multifractality) have been demonstrated for an invertebrate fishery. Previous studies conducted on invertebrate fisheries found monofractal spatial patterns (e.g., fractality in the spatial variability of catch rates and abundance estimates from the northern prawn fishery in Australia (Wang et al. 1999) and from the krill fishery in the Southern Ocean (McClatchie et al. 1994)). Monofractal patterns have also been found in interannual growth rates and recruitment time series of several fish and invertebrate stocks (Niwa 2006, 2007). However, these studies focused only on the estimation of the Hurst parameter to quantify the long-range correlation structure in these time series and did not consider the possible existence of multiple scaling patterns that could produce more complex dynamics. Our findings support those reported by Montes (2004), who analyzed the temporal multifractal dynamics of catches and catch per unit effort from the southern hake fishery in southern Chile. This pattern of self-similar temporal dynamics may be a widespread feature of fisheries, at least in the eastern Pacific Ocean, and not restricted to specific ecosystems or particular fisheries.

Our results demonstrate the existence of multifractal dynamics in smooth pink shrimp daily catch time series off Vancouver Island, Canada, with a scaling range of 16–120 fishing days. This scaling range suggests that different processes affect and structure the availability and (or) catchability of *P. jordani* at time scales less than 120 fishing days, compared with longer time scales. As different segments of the TDCa time series have different scaling properties, the simplest explanation is that low and high catches are regulated by different mechanisms rather than a single mechanism. Several mechanisms have been proposed to explain the emergence of fractal-like spectra in the abundance variability of terrestrial and aquatic populations, including fish stocks, at an interannual scale. For example, age structure, density dependence, measurement errors, and the interaction between age structure and stochastic recruitment are factors used to explain the predominance of low-frequency over high-frequency variability (e.g., Akçakaya et al. 2003; Bjørnstad et al. 2004; Halley and Inchausti 2004) that leads to the appearance of long-range correlations and the characteristic linear trend given by eq. 3 of the power spectrum plot. However, according to our results, intraseasonal time scales of variability play major roles in structuring the scaling dynamics in this pink shrimp fishery. The fractal approach recognizes intermediate scales of variability in this fishery (i.e., from weeks to a season) as fundamental in the emergence of multiple scaling patterns in pink shrimp catches.

Note that only fishing days were analysed over the main fishing seasons from 1994 to 1996. Since TDCr was demonstrated to be a stationary time series across these three fishing seasons, the patterns of variability in any one season are consistent with those in the other seasons, despite the intervening November to March calendar (and nonfishing) days. As a consequence, the interpretation of the processes underlying the 16 to 120 fishing days scaling range apply to the spring to fall fishing seasons.

Potential applications of fractal models in the pink shrimp fishery

For a multifractal time series, the scaling symmetry can be used to predict the probabilities of extreme events at time scales beyond the longest available or at magnitudes in excess of those in the current observations (e.g., Finn et al. 2001). In this latter case, the scaling of the time series involves the preliminary estimation of H, α, and C_1. For example, using the multiple scaling patterns observed for the pink shrimp total daily catch time series, it is possible to predict the probability of achieving values two, three, or other multiples of the observed mean for this time series (e.g., Schertzer et al. 1997; Finn et al. 2001). In terms of its application to the management of this fishery, such predictions of extreme variability can be used to assist fisheries managers with explaining and interpreting occasional very large catches. More detailed information about the multifractal theory used for the prediction of extreme events can be found, for example, in Schertzer et al. (1997) and Finn et al. (2001).

Up until 1997, the pink shrimp fishery along the west coast of Vancouver Island was managed primarily by seasonal closures. Since 2000, management approaches have included preliminary catch ceilings based on preseason biomass forecasts and the application of predetermined harvest rates, followed by reassessment and revision of total allowable catches after completion of fishery-independent biomass surveys (Rutherford et al. 2004; Fisheries and Oceans Canada 2011). When the total allowable catch for a particular area is reached, that area is closed. It is not known at the start of a season whether or when a particular area may reach its quota and be closed. The universal multifractal parameters H, α, and C_1 can be used to construct fractal algo-

rithms (Schertzer et al. 1997) to forecast total daily catch values at intra-annual time scales. These algorithms take into account the extreme fluctuations and the scaling symmetry of multifractal time series and can substantially reduce the forecast errors of individual data points (Richards 2004). In addition, the multiple scaling patterns for this time series can potentially provide an in-season estimate of the future variability of catches using historical data and observations from the early part of the season. Taken together, these properties could provide an early season estimate of when the catch ceiling may be reached in an area and the variability (i.e., uncertainty) around this date (assuming that the fishery and environmental conditions proceed as they have in the past). Traditionally, short-range memory models (ARIMA) have been used in fisheries research to obtain forecast values of catches (Ryall et al. 1999; Hanson et al. 2006; Tsitsika et al. 2007) or a long-memory parameter is used to analyze the dynamics of catches (García et al. 2010), but these fail to represent the extreme variability of catches on a daily scale. In addition, if the observed patterns of variability differ from the predicted patterns, it may indicate that something has changed in the underlying processes governing daily catches, thereby serving as an early warning indicator of these changing conditions.

By using fractal and multifractal models it is also possible to detect the degree of association between fisheries and oceanographic time series in a more formal way than using classical correlation analyses. This new correlation function based on multifractal theory has desirable properties: (*i*) no assumptions about the probability distribution of each time series are made, (*ii*) the range of scales for which a significant correlation is found is detected, taking into account the scaling symmetry of each time series, and is not imposed (as usually done) prior to the analysis, (*iii*) the degree of association is calculated considering different intensity levels (by using different statistical moments q) and not only the mean of each time series (Seuront and Schmitt 2005*a*). This latter property can be used to track the evolution of the correlation between two time series. For example, in a hypothetical fish population high catches can be positively correlated with high and intermediate levels of sea surface temperature (SST), but not be associated at all or negatively correlated with low values of SST. Detailed examples of this application in oceanographic research can be found in Seuront and Schmitt (2005*a*, 2005*b*). Preliminary analyses conducted using much longer time series of catches ($N \sim 2500$ observations) confirm the existence of long-range cross-correlations between pink shrimp TDC and SST (not shown here).

Hypotheses for the causes of these fractal patterns

Seasonal scaling patterns may arise from biological processes regulating the abundance and availability of shrimp to these fishing grounds, from behavioural processes within the shrimp fishery itself, from management actions, or a combination of all. Having demonstrated the existence of multifractal temporal patterns in this fishery, ongoing work is focused on quantifying the effects of physical factors and management actions on the dynamics of catches from a fractal perspective. Various hypotheses are being tested and the results will be presented in forthcoming publications. In the following paragraphs we identify some of these hypotheses that may account for the upper scaling limit and multifractality in this fishery.

For biological processes, the upper scaling limit (i.e., 120 fishing days) of the TDCa time series may be associated with the characteristic time scale of seasonal migrations of important predators of these shrimp. Pacific hake (*Merluccius productus*) coastal populations, one of the predators of *P. jordani* (Buckley and Livingston 1997), undertake a south–north seasonal migration through the coastal upwelling domain of the Northeast Pacific for feeding purposes (Beamish et al. 2005). It is not clear how long hake remain in Canadian waters off the west coast of Vancouver Island but they are thought to be present between 80 and 180 days during warm years (Martell 2002). Food web processes relating to the influence of meanders and eddies on phytoplankton production with seasonal time scales of 100–200 days (Henson and Thomas 2007) could also influence the abundance and availability of pink shrimp to the fishery. These values encompass the upper scaling limit (120 fishing days) found for this pink shrimp catch time series, although more evidence is necessary to support these hypotheses.

In regards to processes within the fishery itself, the combined effect of multiple factors like an increase in the abundance of shrimp (Rutherford et al. 2004) and an increase of fishing effort (Fisheries and Oceans Canada 2001) may explain the emergence of multifractal scaling patterns. Major changes in the level of multifractality in time periods with different fleet-resource dynamics were detected in the southern hake fishery of Chile (Montes 2004). To explore this hypothesis, analyses should be conducted that incorporate, for example, time periods for which the shrimp population and fishing effort were more homogeneously distributed compared with those periods when substantial declines in abundance occurred.

Socio-economic factors can have an effect on the selection of fishing grounds and on the behaviour of a trawl fleet (Walters and Martell 2004), which can cause short-range correlations. For example, in the case of rose shrimp (*Aristeus antennatus*) in the northwest Mediterranean, the better knowledge of shrimp distributions obtained by the fleet in the course of the week and higher prices obtained by the fishermen at the end of each week were proposed to explain significant short-range autocorrelations in catch rates at a time lag of 5 days (Sardà and Maynou 1998). In our study, scaling breaks were detected for pink shrimp total daily catch time series at 3 fishing days, which may reflect the effect of fishing location and the duration of the fishing trips. For the *P. jordani* fishery off the coast of California, the locations of fishing on any given day were determined in part by high catches the previous day (Eales and Wilen 1986). In this latter study, fishers used this information to choose the same fishing location until the high density of shrimp was reduced. In the case of the Pacific hake fishery off the west coast of North America, fishing persisted at a specific location for 3–4 days (Dorn 2001). These examples suggest that socio-economic factors may have an effect on the variability of catches but restricted to time scales no greater than a week.

For the *P. jordani* fishery off the west coast of Vancouver Island, wind stress and tidal speed, among other environmental factors, can affect the availability of this species on a time scale of 8–10 days (Perry et al. 2000). This scale is some-

what shorter than the range obtained in this study (16 to 120 fishing days); however, this does not mean that environmental variability has no effect on the availability on *P. jordani* on longer time scales. In the study conducted by Perry et al. (2000), using data from 1996, the variability in catch rates of *P. jordani* was analyzed up to a maximum of 90 days, and indeed, low frequency oscillations in catch rates were found at 30–40 days.

Our ultimate goal is to identify underlying processes that may be sources of the observed fractal properties, as a guide to understanding catch fluctuations and to improve the management of this fishery. These scaling patterns could be used to construct early warning indicators of change in this, and possibly other, fisheries. However, fractality needs to be demonstrated for other fisheries operating in the same and other ecosystems to determine its generality and to be accepted as an early warning fisheries indicator. Considering the increasing monitoring activities of fisheries operations, including on-board observers, the fine resolution data necessary to detect and quantify scaling patterns should become more readily available. Here, we have demonstrated the existence of multiple scaling patterns in pink shrimp catch time series off the west coast of Vancouver Island, which is the necessary first step to demonstrate the ubiquity of fractal patterns in fisheries time series. Having identified such properties in this study, forthcoming papers will analyze longer time series of smooth pink shrimp catches, including periods with different management actions and abundance levels, to examine the use of these properties as early indicators of changes in fisheries.

Acknowledgements

We are grateful to the anonymous reviewers and the Associate Editor for their comments and suggestions that substantially improved this manuscript and to Dan Clarke for discussions on the potential management applications. Funding for this research was provided by the Graduate Entrance Scholarship (GES) and the University Graduate Fellowship (UGF) of The University of British Columbia awarded to R.M.M. and from NSERC (Discovery Grants Program) awarded to E.A.P.

References

Abry, P., Gonçalves, P., and Véhel, J.L. 2009. Scaling, fractals and wavelets. Wiley-ISTE Ltd., London, UK.

Akçakaya, H.R., Halley, J.M., and Inchausti, P. 2003. Population-level mechanisms for reddened spectra in ecological time series. J. Anim. Ecol. **72**(4): 698–702. doi:10.1046/j.1365-2656.2003.00738.x.

Azovsky, A.I., Chertoprood, M.V., Kucheruk, N.V., Rybnikov, P.V., and Sapozhnikov, F.V. 2000. Fractal properties of spatial distribution of intertidal benthic communities. Mar. Biol. **136**(3): 581–590. doi:10.1007/s002270050718.

Beamish, R.J., McFarlane, G.A., and King, J.R. 2005. Migratory patterns of pelagic fishes and possible linkages between open ocean and coastal ecosystems off the Pacific coast of North America. Deep Sea Res. Part II Top. Stud. Oceanogr. **52**(5–6): 739–755. doi:10.1016/j.dsr2.2004.12.016.

Bjørnstad, O., Nisbet, R.M., and Fromentin, J.M. 2004. Trends and cohort resonant effects in age-structured populations. J. Anim. Ecol. **73**(6): 1157–1167. doi:10.1111/j.0021-8790.2004.00888.x.

Boutillier, J.A., Perry, R.I., Waddell, B., and Bond, J. 1997. Assessment of the offshore *Pandalus jordani* trawl fishery off the west coast of Vancouver Island. Pacific Stock Assessment Review Committee (PSARC) Working Paper No. I-97-11.

Buckley, T.W., and Livingston, P.A. 1997. Geographic variation in the diet of Pacific hake, with a note on cannibalism. CalCOFI Rep. **38**: 53–62.

Burnham, K.P., and Anderson, D.R. 2002. Model selection and multimodel inference. A practical information-theoretic approach. Second ed. Springer-Verlag, New York.

Butler, T.H. 1980. Shrimps of the Pacific coast of Canada. Can. Bull. Fish. Aquat. Sci. No. 202.

Chamoli, A., Bansal, A.R., and Dimri, V.P. 2007. Wavelet and rescaled range approach for the Hurst coefficient for short and long time series. Comput. Geosci. **33**(1): 83–93. doi:10.1016/j.cageo.2006.05.008.

Crawley, M.J. 2007. The R book. John Wiley & Sons, Chichester, UK.

Cryer, J.D., and Chan, K.-S. 2008. Time series analysis with applications in R. 2nd ed. Springer Science+Business Media, LCC, New York.

Davis, A., Marshak, A., Wiscombe, W., and Cahalan, R. 1994. Multifractal characterization of nonstationarity and intermittency in geophysical fields: observed, retrieved, or simulated. J. Geophys. Res. **99**(D4): 8055–8072. doi:10.1029/94JD00219.

Davis, A., Marshak, A., Wiscombe, W., and Cahalan, R. 1996. Multifractal characterizations of intermittency in nonstationary geophysical signals and fields. A model based perspective on ergodicity issues illustrated with cloud data. *In* Currents topics in nonstationary analysis. *Edited by* G. Treviño, J. Hardin, B. Douglas, and E. Andreas. World-Scientific, Singapore. pp. 97–158.

Delignieres, D., Ramdani, S., Lemoine, L., Torre, K., Fortes, M., and Ninot, G. 2006. Fractal analyses for 'short' time series: a re-assessment of classical methods. J. Math. Psychol. **50**(6): 525–544. doi:10.1016/j.jmp.2006.07.004.

Dorn, M.W. 2001. Fishing behavior of factory trawlers: a hierarchical model of information processing and decision-making. ICES J. Mar. Sci. **58**(1): 238–252. doi:10.1006/jmsc.2000.1006.

Downton, M.W., and Miller, K.A. 1998. Relationships between Alaskan salmon catch and North Pacific climate on interannual and interdecadal time scales. Can. J. Fish. Aquat. Sci. **55**(10): 2255–2265. doi:10.1139/f98-106.

Eales, J., and Wilen, J.E. 1986. An examination of fishing location choice in the pink shrimp fishery. Mar. Resour. Econ. **2**: 331–351.

Efron, B., and Tibshirani, R.J. 1993. An introduction to the bootstrap. Monographs on statistics and applied probability 57. Chapman & Hall/CRC, Boca Raton, Fla.

Finn, D., Lamb, B., Leclerc, M.Y., Lovejoy, S., Pecknold, S., and Schertzer, D. 2001. Multifractal analysis of line-source plume concentration fluctuations in surface-layer flows. J. Appl. Meteorol. **40**(2): 229–245. doi:10.1175/1520-0450(2001)040<0229:MAOLSP>2.0.CO;2.

Fisher, K.E., Wiebe, P.H., and Malamud, B.D. 2004. Fractal characterization of local hydrographic and biological scales of patchiness on Georges Bank. *In* Handbook of scaling methods in aquatic ecology: measurements, analysis, simulation. *Edited by* L. Seuront and P.G. Strutton. CRC Press, Boca Raton, Fla. pp. 297–319.

Fisheries and Oceans Canada. 2001. Fish stocks of the Pacific Coast. Fisheries and Oceans Canada, Nanaimo, B.C., Canada.

Fisheries and Oceans Canada. 2011. Pacific Region, Integrated Fisheries Management Plan, shrimp by trawl, April 1, 2011 to March 31, 2012 [online]. Available from http://www.dfo-mpo.gc.ca/Library/343050.pdf [accessed 26 September 2011].

Gao, J., Hu, J., Tung, W.-W., Cao, Y., Sarshar, N., and Roychowdhury, V.P. 2006. Assessment of long-range correlation

in time series: how to avoid pitfalls. Phys. Rev. E, **73**(1): 016117. doi:10.1103/PhysRevE.73.016117.

García, J., Arteche, J., and Murillas, A. 2010. Fractional integration analysis and its implications on profitability: the case of the mackerel market in the Basque Country. Fish. Res. **106**(3): 420–429. doi:10.1016/j.fishres.2010.09.015.

Goldberger, A.L., Amaral, L.A.N., Hausdorff, J.M., Ivanov, P.Ch., Peng, C.-K., and Stanley, H.E. 2002. Fractal dynamics in physiology: alterations with disease and aging. Proc. Natl. Acad. Sci. U.S.A. **99**(Suppl. 1): 2466–2472. doi:10.1073/pnas.012579499.

Guichard, F., Halpin, P.M., Allison, G.W., Lubchenco, J., and Menge, B.A. 2003. Mussel disturbance dynamics: signatures of oceanographic forcing from local interactions. Am. Nat. **161**(6): 889–904. doi:10.1086/375300.

Halley, J.M., and Inchausti, P. 2004. The increasing importance of 1/f noises as models of ecological variability. Fluct. Noise Lett. **4**: R1–R26.

Halley, J.M., and Stergiou, K.I. 2005. The implications of increasing variability of fish landings. Fish Fish. **6**: 266–276.

Hanson, P.J., Vaughan, D.S., and Narayan, S. 2006. Forecasting annual harvests of Atlantic and Gulf menhaden. N. Am. J. Fish. Manage. **26**(3): 753–764. doi:10.1577/M04-096.1.

Henson, S.A., and Thomas, A.C. 2007. Phytoplankton scales of variability in the California Current System: 2. Latitudinal variability. J. Geophys. Res. **112**: C07018. doi:10.1029/2006JC004040.

Hilborn, R., and Mangel, M. 1997. The ecological detective. Confronting models with data. Princeton University Press, Princeton, N.J.

Journel, A.G., and Huijbregts, C.J. 1978. Mining geostatistics. Academic Press, London, UK.

Kiyani, K.H., Chapman, S.C., and Watkins, N.W. 2009. Pseudononstationarity in the scaling exponents of finite-interval time series. Phys. Rev. E, **79**(3): 036109.

Kravchenko, A.N., Boast, Ch.W., and Bullock, D.G. 1999. Multifractal analysis of soil spatial variability. Agron. J. **91**(6): 1033–1041. doi:10.2134/agronj1999.9161033x.

Lavallée, D., Lovejoy, S., Schertzer, D., and Ladoy, P. 1993. Nonlinear variability of landscape topography: multifractal analysis and simulation. *In* Fractals in geography. *Edited by* N. Lam and L. De Cola. Prentice Hall, Englewood Cliffs, N.J., USA. pp. 158–192.

Lovejoy, S., Currie, W.J.S., Tessier, Y., Claereboudt, M.R., Bourget, E., Roff, J.C., and Schertzer, D. 2001. Universal multifractals and ocean patchiness: phytoplankton, physical fields and coastal heterogeneity. J. Plankton Res. **23**(2): 117–141. doi:10.1093/plankt/23.2.117.

Mandelbrot, B.B. 1983. The fractal geometry of nature. W.H. Freeman & Co., San Francisco, Calif.

Mandelbrot, B.B., and Van Ness, J.W. 1968. Fractional Brownian motion, fractional noises, and applications. SIAM Rev. **10**(4): 422–437. doi:10.1137/1010093.

Martell, S.J.D. 2002. Variation in pink shrimp populations off the west coast of Vancouver Island: oceanographic and trophic interactions. Ph.D. thesis, Department of Zoology, The University of British Columbia, Vancouver, B.C.

McClatchie, S., Greene, Ch.H., Macaulay, M.C., and Sturley, D.R.M. 1994. Spatial and temporal variability of Antarctic krill: implications for stock assessment. ICES J. Mar. Sci. **51**(1): 11–18. doi:10.1006/jmsc.1994.1002.

Montanari, A., Taqqu, M.S., and Teverovsky, V. 1999. Estimating long-range dependence in the presence of periodicity: an empirical study. Math. Comput. Model. **29**(10–12): 217–228. doi:10.1016/S0895-7177(99)00104-1.

Montes, R.M. 2004. Fractality and multifractality in the temporal dynamics of a fishery: the case of the southern hake (*Merluccius australis*). M.Sc. thesis, Department of Oceanography, University of Concepción, Concepción, Chile.

Niwa, H.-S. 2006. Recruitment variability in exploited aquatic populations. Aquat. Living Resour. **19**(3): 195–206. doi:10.1051/alr:2006020.

Niwa, H.-S. 2007. Random-walk dynamics of exploited fish populations. ICES J. Mar. Sci. **64**(3): 496–502. doi:10.1093/icesjms/fsm004.

Pascual, M., Ascioti, F.A., and Caswell, H. 1995. Intermittency in the plankton: a multifractal analysis of zooplankton biomass variability. J. Plankton Res. **17**(6): 1209–1232. doi:10.1093/plankt/17.6.1209.

Percival, D.B., Overland, J.E., and Mofjeld, H.O. 2001. Interpretation of North Pacific variability as a short-and long-memory process. J. Clim. **14**(24): 4545–4559. doi:10.1175/1520-0442(2001)014<4545:IONPVA>2.0.CO;2.

Perry, R.I., Boutillier, J.A., and Foreman, M.G.G. 2000. Environmental influences on the availability of smooth pink shrimp, *Pandalus jordani*, to commercial fishing gear off Vancouver Island, Canada. Fish. Oceanogr. **9**(1): 50–61. doi:10.1046/j.1365-2419.2000.00121.x.

Pyper, B.J., and Peterman, R.M. 1998. Comparison of methods to account for autocorrelation in correlation analyses of fish data. Can. J. Fish. Aquat. Sci. **55**(9): 2127–2140. doi:10.1139/f98-104.

R Development Core Team. 2005. R: a language and environment for statistical computing [online]. R Foundation for Statistical Computing, Vienna, Austria. Available from http://www.R-project.org.

Richards, G.R. 2004. A fractal forecasting model for financial time series. J. Forecast. **23**(8): 586–601. doi:10.1002/for.927.

Rodriguez-Iturbe, I., and Rinaldo, A. 2001. Fractal river basins. Chance and self-organization. Cambridge University Press, New York.

Rutherford, D.T., Barton, L.L., Gillespie, G.E., and Boutillier, J.A. 2004. Utility of historical catch data in setting reference points for the British Columbia shrimp by trawl fishery. Canadian Science Advisory Secretariat, Ottawa, Ont. Res. Doc. 2004/026.

Ryall, P., Murray, C., Palermo, V., Bailey, D., and Chen, D. 1999. Status of clockwork chum salmon stock and review of the clockwork management strategy. Canadian Stock Assessment Secretariat, Ottawa, Ont. Res. Doc. 1999/169.

Samorodnitsky, G., and Taqqu, M.S. 1994. Stable non-Gaussian random processes. Stochastic models with infinite variance. Chapman and Hall/CRC, Boca Raton, Fla.

Sardà, F., and Maynou, F. 1998. Assessing perceptions: do Catalan fishermen catch more shrimp on Fridays? Fish. Res. **36**(2–3): 149–157. doi:10.1016/S0165-7836(98)00102-7.

Schertzer, D., and Lovejoy, S. 1987. Physical modeling and analysis of rain and clouds by anisotropic scaling multiplicative processes. J. Geophys. Res. **92**(D8): 9693–9714. doi:10.1029/JD092iD08p09693.

Schertzer, D., Lovejoy, S., Schmitt, F., Chigirinskaya, Y., and Marsan, D. 1997. Multifractal cascade dynamics and turbulent intermittency. Fractals, **5**(3): 427–471. doi:10.1142/S0218348X97000371.

Schmid, P.E. 2000. Fractal properties of habitat and patch structure in benthic ecosystems. *In* Advances in ecological research **30**. *Edited by* A.H. Fitter and D.G. Raffaelli. Academic Press, London, UK. pp. 339–401.

Seuront, L. 2010. Fractals and multifractals in ecology and aquatic science. CRC Press, Boca Raton, Fla.

Seuront, L., and Lagadeuc, Y. 2001. Multiscale patchiness of the

calanoid copepod *Temora longicornis* in a turbulent coastal sea. J. Plankton Res. **23**(10): 1137–1145. doi:10.1093/plankt/23.10.1137.

Seuront, L., and Schmitt, F.G. 2005*a*. Multiscaling statistical procedures for the exploration of biophysical coupling in intermittent turbulence. Part I. Theory. Deep Sea Res. Part II Top. Stud. Oceanogr. **52**(9–10): 1308–1324. doi:10.1016/j.dsr2.2005.01.006.

Seuront, L., and Schmitt, F.G. 2005*b*. Multiscaling statistical procedures for the exploration of biophysical coupling in intermittent turbulence. Part II. Applications. Deep Sea Res. Part II Top. Stud. Oceanogr. **52**(9–10): 1325–1343. doi:10.1016/j.dsr2.2005.01.005.

Seuront, L., Schmitt, F., Lagadeuc, Y., Schertzer, D., and Lovejoy, S. 1999. Universal multifractal analysis as a tool to characterize multiscale intermittent patterns: example of phytoplankton distribution in turbulent coastal waters. J. Plankton Res. **21**(5): 877–922. doi:10.1093/plankt/21.5.877.

Seuront, L., Gentilhomme, V., and Lagadeuc, Y. 2002. Small-scale nutrient patches in tidally mixed coastal waters. Mar. Ecol. Prog. Ser. **232**: 29–44. doi:10.3354/meps232029.

Seuront, L., Brewer, M.C., and Strickler, J.R. 2004. Quantifying zooplankton swimming behavior: the question of scale. *In* Handbook of scaling methods in aquatic ecology. Measurement, analysis, simulation. *Edited by* L. Seuront and P.G. Strutton. CRC Press, Boca Raton, Fla. pp. 333–359.

Takalo, J., Lohikoski, R., and Timonen, J. 1995. Structure function as a tool in AE and Dst time series analysis. Geophys. Res. Lett. **22**(5): 635–638. doi:10.1029/95GL00053.

Tennekoon, L., Boufadel, M.C., and Nyquist, J.E. 2005. Multifractal characterization of airborne geophysical data at the Oak Ridge Facility. Stoch. Env. Res. Risk Assess. **19**(3): 227–239. doi:10.1007/s00477-004-0227-z.

Theil, H. 1972. Statistical decomposition analysis with applications in the social and administrative sciences. North-Holland Publishing Company, Amsterdam, the Netherlands.

Tsitsika, E., Maravelias, Ch., and Haralabous, J. 2007. Modeling and forecasting pelagic fish production using univariate and multivariate ARIMA models. Fish. Sci. **73**(5): 979–988. doi:10.1111/j.1444-2906.2007.01426.x.

Walters, C.J., and Martell, S.J.D. 2004. Fisheries ecology and management. Princeton University Press, Princeton, N.J.

Wang, Y.-G., Lin, Y.-X., and Haywood, M.D.E. 1999. A quasi-likelihood method for fractal-dimension estimation. Math. Comput. Simul. **48**(4–6): 429–436. doi:10.1016/S0378-4754(99)00032-4.

Webster, R., and Oliver, M. 1992. Sample adequately to estimate variograms of soil properties. J. Soil Sci. **43**(1): 177–192. doi:10.1111/j.1365-2389.1992.tb00128.x.

Wilson, P.S., Tomsett, A.C., and Toumi, R. 2003. Long-memory analysis of time series with missing values. Phys. Rev. E, **68**(1): 017103. doi:10.1103/PhysRevE.68.017103.

Xia, X., Lazarou, G.Y., and Butler, T. 2005. Automatic scaling range selection for long-range dependent network traffic. IEEE Commun. Lett. **9**(10): 954–956. doi:10.1109/LCOMM.2005.10013.

Yu, C.X., Gilmore, M., Peebles, W.A., and Rhodes, T.L. 2003. Structure function analysis of long-range correlations in plasma turbulence. Phys. Plasmas, **10**(7): 2772–2779. doi:10.1063/1.1583711.

Zar, J.H. 1999. Biostatistical analysis. 4th ed. Prentice Hall, Upper Saddle River, N.J., USA.

ERRATUM / ERRATUM

Erratum: Multifractal patterns in the daily catch time series of smooth pink shrimp (*Pandalus jordani*) from the west coast of Vancouver Island, Canada

Rodrigo M. Montes, R. Ian Perry, Evgeny A. Pakhomov, Andrew M. Edwards, and James A. Boutillier

Ref.: Can. J. Fish. Aquat. Sci. **69**(2): 398–413 (2012).

For Fig. 5 on page 406, the figure shows "5 fishing days time lag". This is incorrect. It should read "15 fishing days time lag". The correct figure is shown below. The publisher apologizes for any inconvenience this might have caused.

Fig. 5. Structure function $Y_r(q)$ versus r in a log–log plot obtained from the pink shrimp (*Pandalus jordani*) total daily catch residual time series (TDCr) for the west coast of Vancouver Island from 1994 to 1996. Two increasing trends, the first between 1 and 3 fishing days and the second between 4 and 15 fishing days, are visible.

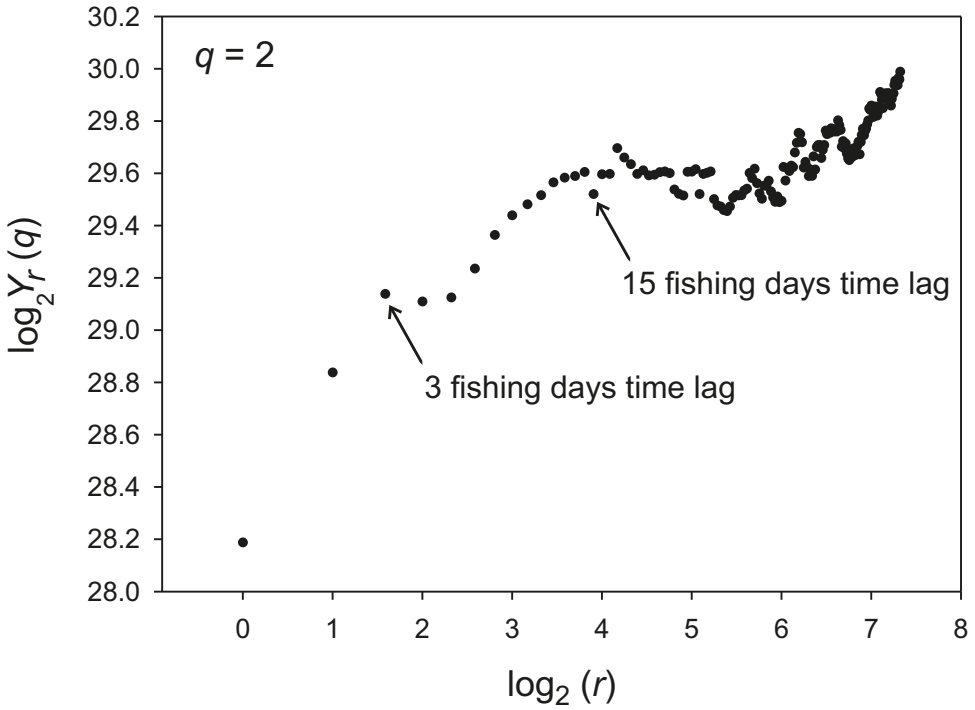

Received 9 February 2012. Accepted 9 February 2012. Published at www.nrcresearchpress.com/cjfas on 17 February 2012. J2011-0015E

R.M. Montes* and E.A. Pakhomov. Department of Earth and Ocean Sciences, The University of British Columbia, 6339 Stores Road, Vancouver, BC V6T 1Z4, Canada.
R.I. Perry, A.M. Edwards, and J.A. Boutillier. Fisheries and Oceans Canada, Pacific Biological Station, 3190 Hammond Bay Road, Nanaimo, BC V9T 6N7, Canada.

Corresponding author: Rodrigo M. Montes (e-mail: rmontes@eos.ubc.ca and rmontes@udec.cl).

*Present address: COPAS Sur-Austral, University of Concepción, Casilla 160-C, Concepción, Chile.